Results from NIMROD/NEO/NIES Benchmark

CEMM Meeting, San Diego, CA

E. Held[1] S. Kruger[2] NIMROD Team

[1]Department of Physics
Utah State University

[2]Tech-X Corp.

March 23, 2014

Electron, ion and hot particle DKEs in NIMROD

- Consider Hazeltine's form for the first-order drift kinetic equation in energy, ε, and magnetic moment, μ, variables:

$$\partial_t f + (\mathbf{v}_{||} + v_D) \cdot \nabla f + \left(\mu \frac{\partial B}{\partial t} + e(\mathbf{v}_{||} + \mathbf{v}_D) \cdot \mathbf{E} \right) \partial_\varepsilon f = C.$$

- Transforming to pitch-angle, $\xi = v_{||}/v$, and normalized speed, $s = v/v_0$, variables yields

$$\partial_t f + (\mathbf{v}_{||} + \mathbf{v}_D) \cdot \nabla f + \frac{s}{2} \Big[-(\mathbf{v}_{||} + \mathbf{v}_D) \cdot \nabla \ln T_0 - (1 - \xi^2) \frac{\mathbf{b}}{B} \cdot \nabla \times \mathbf{E} + \frac{e}{s^2 T_0} (\mathbf{v}_{||} + \mathbf{v}_D) \cdot \mathbf{E} + (1 + \xi^2) \frac{\mathbf{E} \times \mathbf{B}}{B^2} \cdot \nabla \ln B \Big] \frac{\partial f}{\partial s} + \frac{1 - \xi^2}{2\xi} \Big[-(\mathbf{v}_{||} + \mathbf{v}_D) \cdot \nabla \ln B + \xi^2 \frac{\mathbf{b}}{B} \cdot \nabla \times \mathbf{E} + \frac{e}{s^2 T_0} (\mathbf{v}_{||} + \mathbf{v}_D) \cdot \mathbf{E} + \xi^2 \frac{\mathbf{E} \times \mathbf{B}}{B^2} \cdot \nabla \ln B \Big] \frac{\partial f}{\partial \xi} = C(f).$$

Coulomb Collision Operator

- Since last Sherwood, implemented full, linearized collision operator using 1D finite-elements in pitch angle and non-classical, orthogonal speed polynomials.
- Expand $F = \sum_l F_l(\mathbf{x}, s, t)\phi_l(\xi) = \sum_{lk} F_{lk}(\mathbf{x}, t) L_k(s)\phi_l(\xi)$ and use in

$$
\begin{aligned}
C_{ab}^{test} &= \Gamma_{ab}\{\frac{1}{2v^3} g_v^0 \mathscr{L}(f) + \frac{1}{v^2} g_v^0 f_v + \frac{1}{2} g_{vv}^0 f_{vv} + (1 - \frac{m_a}{m_b}) h_v^0 f_v + \frac{m_a}{m_b} 4\pi f_b^0 f_a\} \\
C_{ab}^{field} &= \Gamma_{ab}\{\frac{1}{2v^3} f_v^0 \mathscr{L}(g) + \frac{1}{v^2} f_v^0 g_v + \frac{1}{2} f_{vv}^0 g_{vv} + (1 - \frac{m_a}{m_b}) f_v^0 h_v + \frac{m_a}{m_b} 4\pi f_a^0 f_b\}.
\end{aligned}
$$

where $\mathscr{L} = \partial_\xi (1 - \xi^2)\partial_\xi$ and g and h are Rosenbluth potentials.

- NEO uses $F = \sum_{lm} F_{lm}(\mathbf{x}, t) L_m^{k(l)+1/2}(s^2) s^{k(l)} P_l(\xi) f_0$ where $k(l = 0) = 0$ and $k(l > 0) = 1$.

NIMROD benchmark with NEO

- For benchmark, order $v_D << v_{||}$ and assume weak electric fields.
- Lowest-order equation satisfied by a stationary Maxwellian, f_0, parameterized by $n(\psi)$ and $T(\psi)$.

  To next order :

$$\partial_t f_1 + \mathbf{v}_{||}\cdot\nabla f_1 - \left(\mathbf{v}_{||}\cdot\nabla\ln B\right)\frac{1-\xi^2}{2\xi}\partial_\xi f_1 - C_{aa} - C_{ab} \quad =$$

$$-\mathbf{v}_D\cdot\nabla f_0 + s\mathbf{v}_D\cdot\nabla\ln v_0\partial_s f_0 - \frac{e}{2\varepsilon_0 s}\mathbf{v}_{||}\cdot\left(\mathbf{E}^A - \nabla\phi_1\right)\partial_s f_0$$

Using $F = f_1 - (e\phi_1/T_0)f_0$ yields (Belli and Candy, 51 PPCF 2009):

$$\mathbf{v}_{||}\cdot\nabla F - \mathbf{v}_{||}\cdot\nabla\ln B\partial_\xi F - C_{aa}(F) - C_{ab}(F) \quad =$$

$$-\mathbf{v}_D\cdot\nabla f_0 + s\mathbf{v}_D\cdot\nabla\ln v_0\partial_s f_0 - \frac{e}{2\varepsilon_0 s}\mathbf{v}_{||}\cdot\mathbf{E}^A\partial_s f_0$$

This equation is solved for electrons and ions for this benchmark.

High-Beta Benchmark

- T on axis 7.5 KeV.

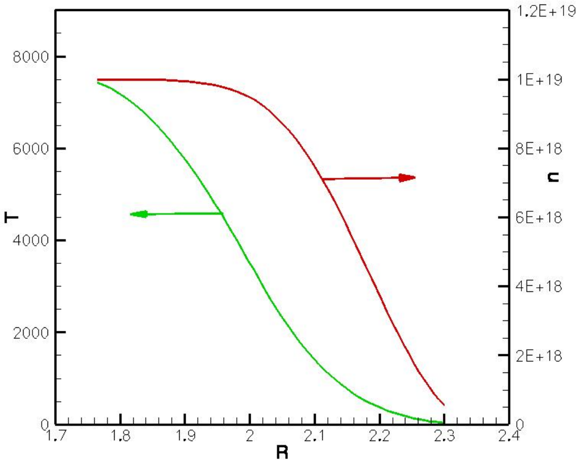

Spatial Grid and q profile

- NIMROD spatial grid has pd=2, mx=32, my=48.
- Reverse shear q profile in core a challenge for velocity space convergence.
- NEO spatial grid has nradial=20 and ntheta=29 for highest resolution case.

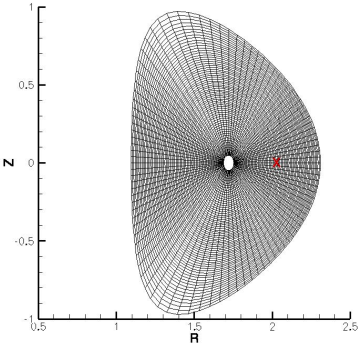

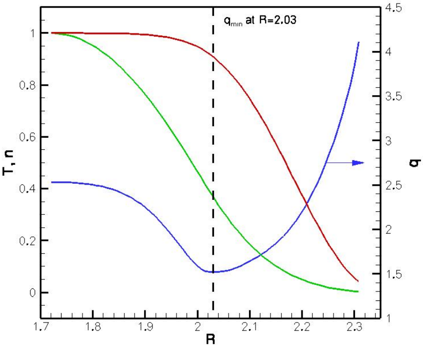

NIMROD Velocity Space Grid

- NIMROD velocity grid has 3 cells in pitch angle, polynomial degree of 15, and ns = 12 for highest resolution case.
- NEO uses 45 Legendre polynomials and 12 associated Laguerre polynomials for highest resolution case.

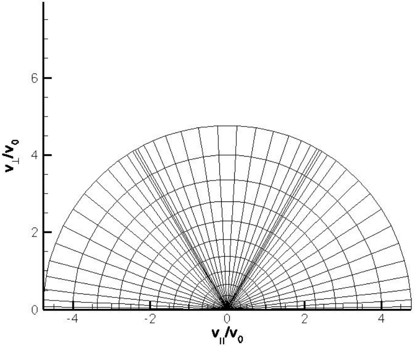

Electron Particle Flux Convergence

- Radial particle fluxes defined as $\Gamma_a = < \int d\mathbf{v} \, [\mathbf{v}_D \cdot \nabla r] \, F_a >$.
- Increasing polynomial degree for NIMROD and number of Legendre polynomials for NEO.

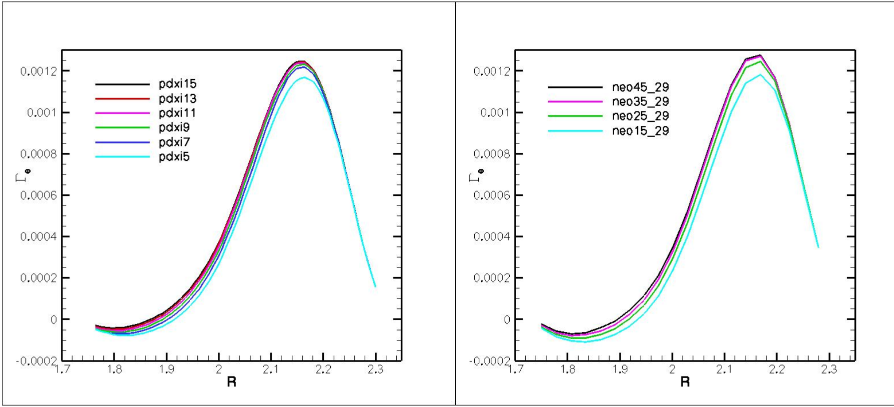

Bootstrap Current Convergence

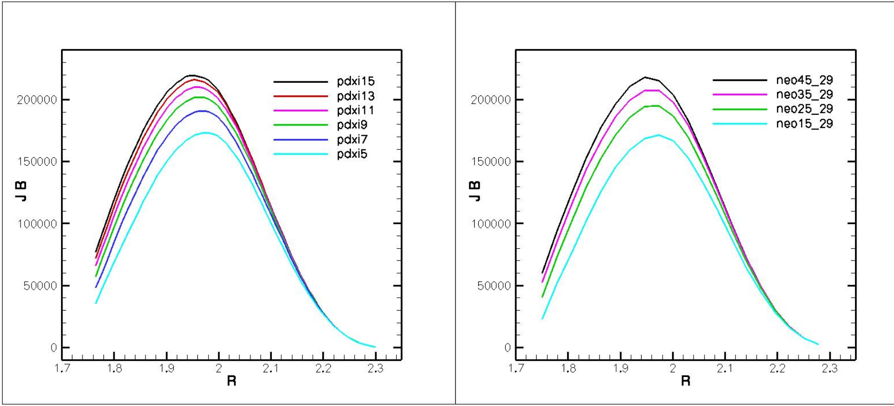

- Radial heat fluxes defined as $Q_a = < \int d\mathbf{v} \frac{1}{2} m v'^2 \left[\mathbf{v}_D \cdot \nabla r \right] F_a >$.

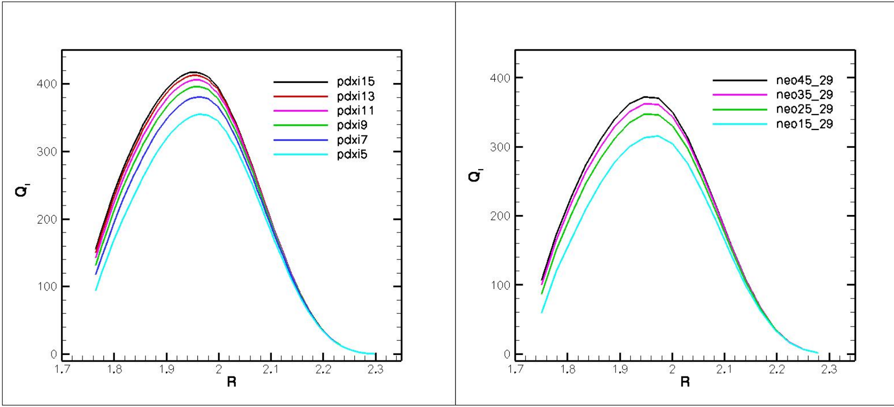

Comparison of Bootstrap Currents

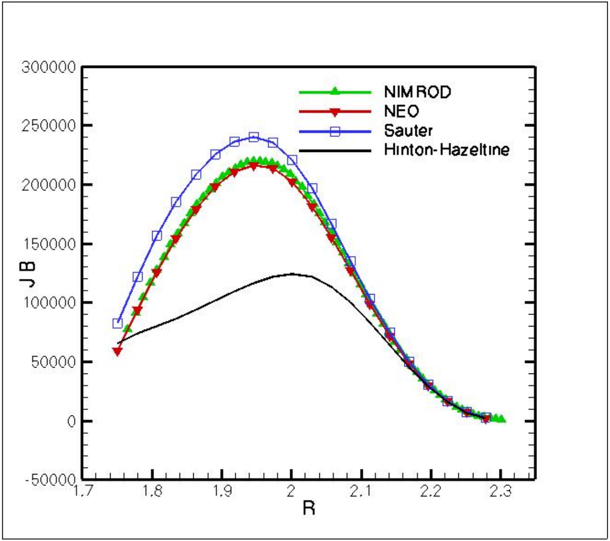

Comparison of Γ_e and Q_i

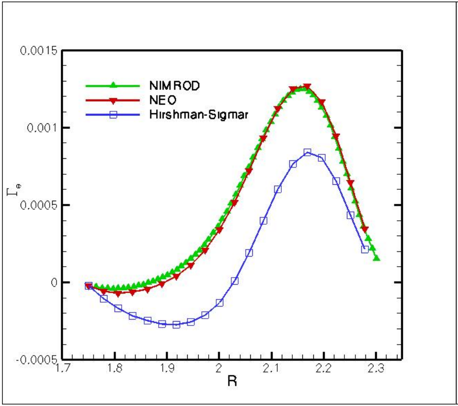

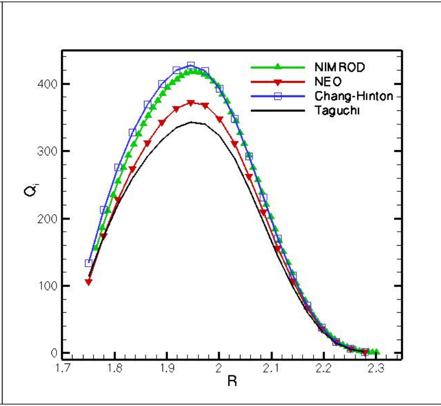

- F_e shown at outboard midplane, R=2.03.

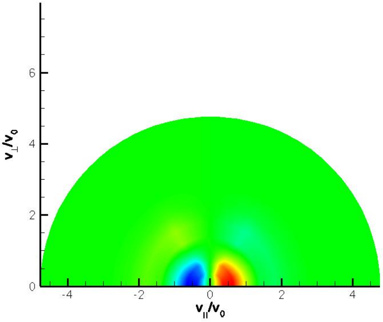

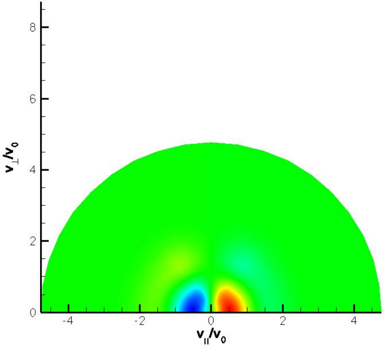

NIMROD and NEO Ion Distribution Functions

- F_i shown at outboard midplane, R=2.03.

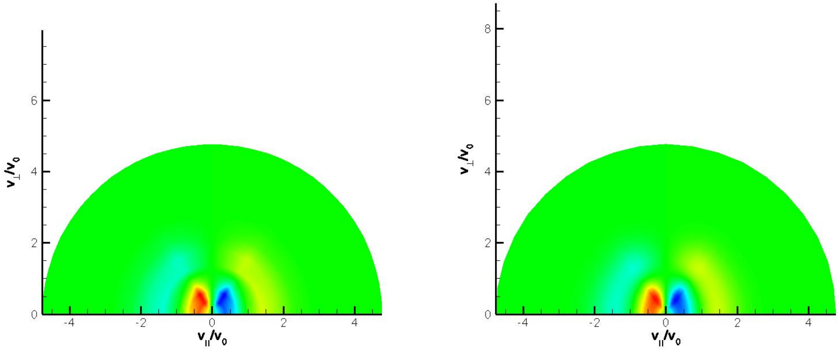

Blow up of NIMROD and NEO Ion Distribution Functions

- F_i shown at outboard midplane, R=2.03.

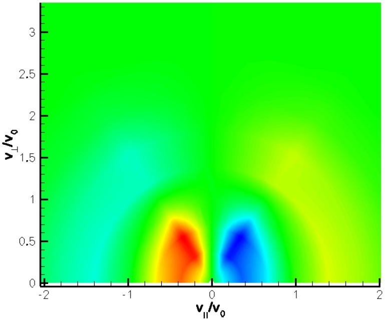

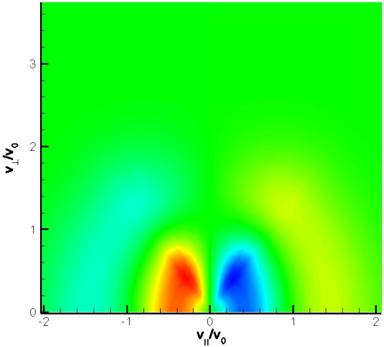

NSTX Benchmark

- NSTX equilibrium provided by Brendan Lyons (Phys. Plasmas 19, 082515 (2012)).

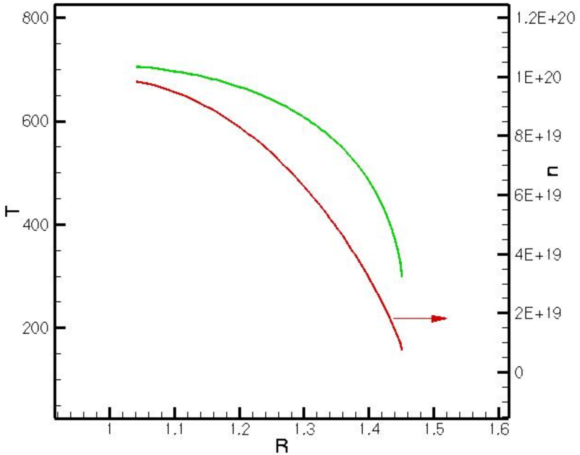

Spatial and Velocity Space Grids

- NIMROD spatial grid has pd=1, mx=64, my=96.
- NIMROD velocity grid has 3 cells, polynomial degree of 11, and ns = 12.

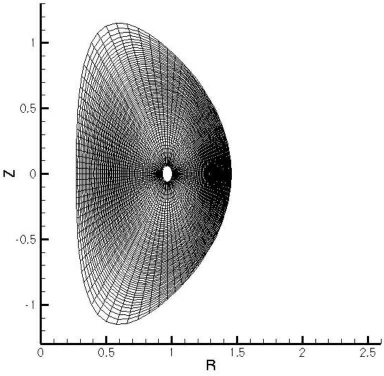

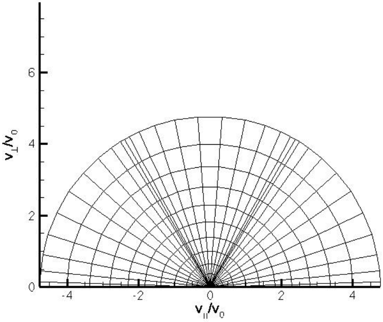

Comparison of NIMROD/NEO/NIES Bootstrap Currents

- Here Sauter (computed from NEO) and NIES solve DKE in $\nu^* = 0$ limit.
- NEO and NIMROD results are at finite ν^*.

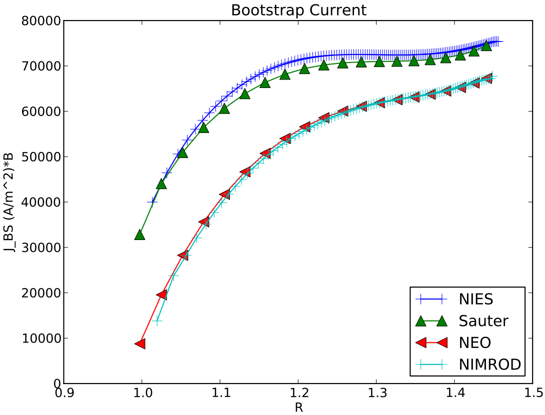

Comparison of NIMROD/NEO/NIES Bootstrap Currents

- Here NIES solves DKE in $\nu^* = 0$ limit.
- Sauter, NEO and NIMROD results are at finite ν^*.

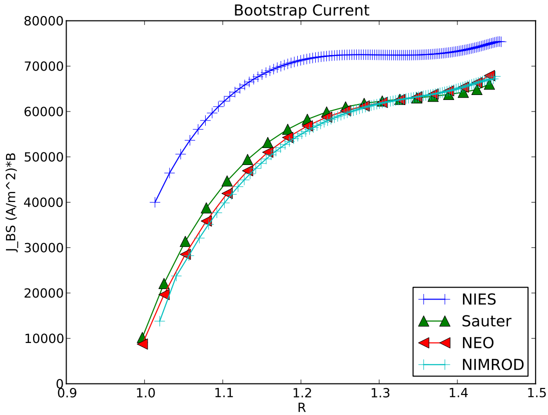

Conclusion

- Quantitative agreement between NIMROD and NEO for
  (1) high aspect ratio circular equilibrium (shown at previous CEMM meeting),
  (2) high-beta, DIII-D like equilibrium, and
  (3) NSTX equilibrium.
- Bootstrap currents consistent for NIES and NEO's Sauter formula in $\nu^* = 0$ limit of NSTX case.
- NIMROD/NEO/Sauter bootstrap currents agree for finite ν^* NSTX case.
- Future work:
  -publish paper on NIMROD/NEO benchmark milestone,
  -resume with continuum hot particles applied to giant sawteeth problem (Schnack).